

Green Chemistry

Accepted Manuscript



This is an *Accepted Manuscript*, which has been through the Royal Society of Chemistry peer review process and has been accepted for publication.

Accepted Manuscripts are published online shortly after acceptance, before technical editing, formatting and proof reading. Using this free service, authors can make their results available to the community, in citable form, before we publish the edited article. We will replace this *Accepted Manuscript* with the edited and formatted *Advance Article* as soon as it is available.

You can find more information about *Accepted Manuscripts* in the [Information for Authors](#).

Please note that technical editing may introduce minor changes to the text and/or graphics, which may alter content. The journal's standard [Terms & Conditions](#) and the [Ethical guidelines](#) still apply. In no event shall the Royal Society of Chemistry be held responsible for any errors or omissions in this *Accepted Manuscript* or any consequences arising from the use of any information it contains.

Understanding the destructurement of starch in water/ionic liquid mixtures

L. S. Sciarini,^{a,c} A. Rolland-Sabaté,^{b,c} S. Guilois,^{b,c} P. Decaen,^{a,b} E. Leroy,^{a,b} P. Le Bail^{b,c}

Abstract

The destructurement of native maize starch in mixtures of water and ionic liquids (IL) containing acetate anions was studied in dynamic heating conditions, combining calorimetry, rheology, microscopy and chromatographic techniques. A phase diagram of starch in water/IL solutions was established. The phase transitions undergone by starch include the typical endothermic gelatinization phenomenon for IL/water ratios lower than 0.5, while for higher ionic liquid content a complex exothermic phenomenon combining mild degradation and solubilization takes place. This results in an optimum destructurement temperature as low as 40-50 °C for an IL/water ratio close to 0.7. In addition, specific macromolecular chain breakings appear to take place, depending on the nature of the cations present, resulting in different macromolecular structures of recovered starch. These results suggest the possibility of solvent media design for a controlled modification of starch macromolecular characteristics.

1. Introduction

As renewable resources are becoming essential for the industry, the creative design and application of innovative technology for the optimization of such resources is a research topic raising a huge interest since the past decade.¹ Among all polysaccharides investigated as potential alternatives to conventional oil based plastics, starch has attracted a large amount of attention.² Starch is one of the most abundant biopolymers

25 in nature, and considering its low cost, renewability, and biodegradability, it can be
26 considered as a raw material for the elaboration of biologically degradable materials.

27 Starch is composed of two different glucose polymers: amylose, a predominantly linear
28 macromolecule formed from $\alpha(1\rightarrow4)$ linkages with a molar mass $\sim 10^5 - 10^6 \text{ g mol}^{-1}$,
29 and amylopectin, a massive multiply branched polymer containing both $\alpha(1\rightarrow4)$ and
30 $\alpha(1\rightarrow6)$ linkages with a molar mass $\sim 10^7 - 10^9 \text{ g mol}^{-1}$. Starch is synthesized in the form
31 of densely packed granules, containing both amorphous and crystalline regions.³ Given
32 its granular structure, starch shows low solubility in any conventional solvent in spite of
33 being highly hydrophilic. However, when suspended and heated in excess water, starch
34 undergoes an order-disorder transition called gelatinization. During this phenomenon,
35 starch granules swell and amylose progressively leaches out of the granule, and the semi-
36 crystalline structure is disrupted. Although some starch molecules are readily solubilized
37 in water, some granule remnants may still be present even after gelatinization has
38 occurred. Thus, starch insolubility represents a problem when trying to obtain
39 homogeneous amorphous materials.

40 In the last years, the performance of ionic liquids (ILs) as solvents for biopolymers has
41 generated lots of interest. ILs are room-temperature molten salts; since they present high
42 thermal stability and are not volatile, it has been reported that they offer an alternative
43 to common organic solvents. For this and because they are easily recyclable and even
44 some of them are biodegradable,⁴ they have been classified as ‘green solvents’. For these
45 reasons, they have attracted enormous attention over the past decade, becoming a very
46 fertile area of research.⁵ Over the last years, the use of ILs to dissolve and process starch
47 has been reported.⁶⁻¹⁰ While first reports focused on ionic liquids containing chlorine
48 anions showed strong depolymerisation of starch, limiting the potential applications,⁹
49 more recent works on acetate based ionic liquids are more promising,⁸ despite no clear

50 evaluation of starch degradation in such systems has been communicated by the authors.
51 In presence of chlorine anions, the macromolecular degradation of starch has been
52 related to acidic hydrolysis of glycosidic bonds.^{6,9,11-13} According to Mateyawa *et al.*⁸
53 the presence of acetate based ionic liquid is likely to avoid such phenomena. The same
54 authors also reported an exothermic transition when starch was heated in pure and
55 concentrated 1-ethyl 3-methylimidazolium acetate (EMIMAc) water solutions and it was
56 proposed that this exothermic transition was due to starch dissolution, without
57 gelatinization. Stevenson *et al.*⁹ reported no enthalpic transition when analysing
58 recovered starch, previously treated with 1-butyl-3-methylimidazolium chloride,
59 suggesting that after heated in ILs, starch is destructured and no further gelatinization
60 can be observed when re-heating in water.

61 As recalled by Brennecke *et al.*¹⁴ one of the major advantages of ILs is that they offer
62 the possibility of being tailored by modifying the chemical structure of the cation and
63 anion moieties. Consequently, in the present work, we propose to focus on the influence
64 of the cation by comparing the thermal destructurement of starch mixed with water and
65 two acetate based ionic liquids: EMIMAc and Cholinium Acetate. This latter presents
66 the advantage of a very low toxicity, choline being an essential nutrient and thus
67 biocompatible.

68

69 **2. Experimental**

70 **2.1. Materials**

71 Regular corn starch (Maritena 100) was purchased from Tate & Lyle (Paris, France),
72 with an initial moisture content of 12%. EMIMAc was produced by BASF, and supplied
73 by Sigma-Aldrich. Before use, both materials were dried with P₂O₅ under vacuum at
74 room temperature for one week. After this time, starch moisture was lower than 3%.

75 Cholinium acetate (CholAc) was synthesized by metathesis reaction.¹⁵ Equivalent
76 amounts (0.06 mol each) of cholinium chloride and potassium acetate (both purchased
77 from Aldrich) were dissolved in absolute ethanol, mixed and stirred for 1 hour at room
78 temperature. A white precipitate of potassium was formed and removed by filtration.
79 Ethanol was evaporated on a rotary evaporator. The CholAc thus produced was freeze-
80 dried prior to use. After purification and freeze-drying, CholAc melting point was 83 °C.
81 For analysis, starch was suspended in aqueous solutions of varying IL concentration
82 (from 0% w/w to 100% w/w IL). Since different starch concentrations were also studied,
83 a phase diagram was prepared.
84 ILs are known to be highly hygroscopic thus sample preparation was carried out in a
85 glove box under dry gas purge.

86

87 **2.2. Methodology**

88 **2.2.1. Micro differential scanning calorimetry (μ DSC).** Mixtures of 20% w/w starch in
89 different solvents were prepared. Solvent composition varied from 0% ILs (pure water),
90 to 100% EMIMAc or 95% CholAc (due to its high melting point, 5% water was added
91 to CholAc; the melting point of CholAc 95% was 53 °C). Appropriate amounts of IL and
92 water were weighted and thoroughly mixed before starch addition. A reference cell was
93 prepared by adding the same water content than in the sample cell. Sample was stirred (50 rpm
94 at room temperature) for 1 h before being heated from 20 °C to 120 °C and cooled from 120 °C
95 to 20 °C in the μ DSC (μ DSC7evo, Setaram, Caluire, France) at a heating/cooling rate of 1 °C
96 min⁻¹. The onset (To), peak (Tp) and conclusion temperatures (Tc), and the enthalpy of the
97 transition (ΔH) were determined using Calisto software (Calisto v1.32 DB v1.33). All mixtures
98 were analysed in duplicates.

99

100 **2.2.2. Macromolecular characterization of samples.** High Performance Size
101 Exclusion Chromatography coupled with Multi-Angle Laser Light Scattering, (HPSEC–
102 MALLS) was used. Starch was suspended in IL/water solutions, and stirred for 1 h.
103 These suspensions were then heated in an oil bath (Ministat 240, Huber, Offenburg,
104 Germany) used to mimic the dynamic heating performed with the μ DSC: from 20 °C to
105 120 °C at 1 °C min⁻¹. After this thermal treatment, samples were DMSO-pretreated,
106 precipitated with ethanol, dried and solubilized by microwave heating under pressure, as
107 previously described by Rolland-Sabaté *et al.*¹⁶ Each sample suspension in water at a
108 concentration of 0.5 g L⁻¹ was heated for 40 s (maximal internal temperature reached:
109 152 °C) at 900 W. Starch solutions were then filtered through 5 μ m Durapore TM
110 membranes (Waters, Bedford, MA, USA). Carbohydrate concentrations were
111 determined by the sulphuric acid-orcinol colorimetric method described by Planchot *et*
112 *al.*¹⁷ Sample recoveries were calculated from the ratio of the initial mass and the mass
113 after filtration. Solutions were immediately injected into the HPSEC–MALLS–system.
114 The equipment and the method used were the same as that described previously.¹⁸ The
115 SEC column was Shodex® KW-802.5 (8 mm ID×30 cm) together with a KW-G guard
116 column (6 mm ID×5 cm) both from Showa Denko K.K. (Tokyo, Japan). They were
117 maintained at 30 °C. The two on-line detectors were a Dawn® Heleos® MALLS system
118 fitted with a K5 flow cell and a GaAs laser, ($\lambda = 658$ nm), supplied by Wyatt Technology
119 Corporation (Santa Barbara, CA, USA,) and a RID-10A refractometer from Shimadzu
120 (Kyoto, Japan). The eluent (Millipore water containing 0.2 g L⁻¹ of sodium azide) was
121 carefully degassed and filtered on-line through Durapore GV (0.1 μ m) membranes from
122 Millipore (Millipore, Bedford, MA, USA), and eluted at 0.5 mL min⁻¹. Sample recovery
123 rates were calculated from the ratio of the mass eluted from the column (integration of

124 the refractometric signal) and the injected mass. These last ones were determined using
125 the sulfuric acid-orsinol colorimetric method.¹⁷

126 \bar{M}_n, \bar{M}_w , the dispersity (\bar{M}_w / \bar{M}_n), the radius of gyration \bar{R}_G (nm) were established using
127 ASTRA® software from WTC (version 6.1 for PC), as previously described by Rolland-
128 Sabaté *et al.*^{16,18} A value of 0.146 ml g⁻¹ was used as the refractive index increment
129 (dn/dc) for glucans and the normalization of photodiodes was achieved using a low
130 molar mass pullulan standard (P20).

131

132 **2.2.3. Rapid Visco Analyser (RVA).** Viscosity properties of starch in different solutions
133 were studied with a Rapid Visco Analyser (RVA-3, Newport Scientific Pty. Ltd.,
134 Australia). Starch suspensions (7.5% w/w) were prepared by weighting the solvent in a
135 canister and adding starch slowly while stirring. The slurry was heated from 20 °C to 95
136 °C while being stirred at 960 rpm for the first 10 s and then at 160 rpm until the assay
137 was completed. The heating rate was 10 °C min⁻¹. It was held at 95 °C for 10 min, and
138 finally cooled to 20 °C at a cooling rate of 6.7 °C min⁻¹. Pasting temperature (Tp), peak
139 viscosity (PV), final viscosity (FV), breakdown (BD) and setback (SB) were obtained
140 from the pasting curve. Samples were assessed in duplicate.

141

142 **2.2.4. Microscopy.** The microstructure of the starch suspended in different ILs solutions
143 before and after the enthalpic transitions was analysed with a light microscope LEICA
144 DMRD. Light, polarized light and differential interference contrast images were
145 obtained. Starch suspensions were prepared in the same way than samples analysed by
146 μ DSC. The appropriate amount of IL, water (when required) and starch were weighted.
147 These mixtures were stirred for 1 h and then heated in an oil bath (Ministat 240, Huber,
148 Offenburg, Germany) at 1 °C min⁻¹ until the corresponding temperature was reached.

149 Samples were then removed from the bath and cooled in an ice bath. The samples were
150 immediately observed under the microscope.

151

152 **2.2.5. Statistical analysis.** Data obtained were statistically treated by variance analysis,
153 while means were compared by the Fisher LSD test at a significance level of 0.05
154 (INFOSTAT statistical software, Facultad de Ciencias Agropecuarias, Universidad
155 Nacional de Cordoba, Argentina).

156

157 **3. Results and discussion**

158 **3.1. Differential Scanning Calorimetry (μ DSC)**

159 The thermal behaviour of starch mixed with aqueous ILs solutions of different
160 concentrations was monitored by μ DSC (Figure 1). Increasing concentrations of ILs
161 were used from the bottom to the top of the Figure. When IL concentration was low,
162 starch underwent a typical gelatinization, represented by an endothermic transition (a
163 second endothermic transition can be observed at around 100 °C, and it is ascribed to
164 the melting of amylose-lipid complexes). The fact that gelatinization shifts to higher
165 temperatures with increasing IL concentration is consistent with the previously
166 described effect of the presence of different salts in aqueous solution.^{19,20} The effect of
167 salts on starch gelatinization has been found to follow the Hofmeister series, with
168 kosmotropes (structure making, salting-out) delaying gelatinization and chaotropes
169 (structure breaker, salting-in) accelerating it. Acetate is a well-known kosmotrope, so it
170 was expected to produce a shift of gelatinization toward higher temperatures.
171 Nevertheless, a further increase in IL concentration (up to 50% for EMIMAc and 60%
172 for CholAc) led to a decrease in gelatinization temperature. This trend will be discussed
173 below (see *Macromolecular characteristics*).

174 If we now consider high ILs concentrations (from the top to the bottom, Figure 1) an exothermic
175 transition is present (the highest CholAc concentration studied was 95%, but these results were
176 not included in the Figure since the exothermic peak was not complete at
177 120 °C, which is the upper limit for the μ DSC, but peak onset temperature can be observed in
178 Table 1). This exotherm starts at lower temperatures when water is added, and the heat released
179 (ΔH) is also decreased. There is a critical concentration (depending on the IL used) where both
180 transitions (exo and endothermic) take place: CholAc 70% and EMIMAc 60%. In the former
181 case, both transitions can be observed, but in the latter both phenomena seem to happen at very
182 close temperatures thus probably cancelling one another.

183 The same behaviour was also observed by Mateyawa *et al.*⁸ working with EMIMAc and by
184 Koganti *et al.*²¹ using N-methyl morpholine N-oxide (NMMO). These authors attributed the
185 exothermic transition to starch dissolution in these solvents. Enthalpy values for the exotherm
186 for normal corn starch in NMMO were 17.5 J g⁻¹ (no enthalpy change was observed when
187 increasing NMMO concentration from 70 to 78%), whereas Mateyawa *et al.*⁸ did not provide
188 any ΔH value. In the present study, ΔH of exothermic transition ranged between 17.3 J g⁻¹ (70%
189 EMIMAc) and 180.7 J g⁻¹ (100% EMIMAc) (Table 1). Moreover, when heating at low rates
190 (0.1 °C min⁻¹), two peaks were clearly observed by μ DSC (data presented in supplementary
191 material section, Figure S1); this finding indicates that more than a single phenomenon would
192 be responsible for the exothermic transition. The same trends were observed at different
193 starch/solvent ratio (data not shown).

194

195 **3.2. Macromolecular characterization of treated starches**

196 In order to understand the phenomena underlying the exothermic transition, macromolecular
197 properties of starch treated with ILs were studied using HPSEC-MALLS system. To this end,
198 starch was treated with different IL/water solutions, recovered and DMSO-pre-treated. The

199 DMSO pre-treatment recoveries were between 95 and 100% for all samples. DMSO pre-
200 treatment is known to remove the polysaccharide oligomers with degree of polymerization (DP)
201 lower than 12. Thus, this high recovery percentage shows that the heating of samples in
202 different IL solutions does not induce the apparition of sugars with DP smaller than 12. The
203 solubilisation recovery rates and the elution recoveries of starches were higher than 90%. The
204 high sample recovery values obtained here indicate that the fractionation response was
205 quantitative for all the samples. Overall, this solubilisation procedure was thus considered as
206 enabling the structural characterization of these samples.

207 Figure 2a presents chromatograms for starch heated in pure water and in EMIMAc
208 solutions. When considering starch heated in pure water, two peaks were observed for
209 the differential refractive index signal (corresponding to chains concentration). The first
210 and bigger one (Peak I, 5.8 mL) corresponds to amylopectin population, while the
211 second, and smaller, to amylose (Peak II, 6.6 mL). When analysing starch/EMIMAc
212 100% chromatogram, two peaks are also observed; nevertheless, some important
213 differences can be highlighted: 1) the first peak started to elute at higher volumes,
214 indicating a lower size for these molecules as the elution volume is inversely
215 proportional to the molecular size, 2) the second peak is bigger than the first one, and 3)
216 no evident shift in peak II is observed. In addition the molar mass is clearly lower for
217 each fraction of starch/EMIMAc 100% compared to starch/pure water solutions.
218 Overall, these features indicate that amylopectin is depolymerized when heated in
219 EMIMAc, this explains the shift of amylopectin peak (which accounts for a smaller size),
220 while there is a co-elution of the depolymerisation products and amylose, thus explaining
221 the increased area of the second peak. Finally, no evidence of amylose depolymerisation
222 is found (no shift of the peak II). For samples treated with EMIMAc 70%, amylopectin
223 also eluted at higher volumes, although the overall profile and molar mass distribution

224 are more similar to that of pure water. For EMIMAc 50%, no shift of amylopectin peak
225 was observed, but the area of the peak II is bigger than for starch treated with water,
226 indicating the presence of amylopectin depolymerisation products. Nevertheless, since
227 mild depolymerisation occurs under these conditions (Table 2) the detector response to
228 amylopectin is still high.

229 For the starch heated in 95% CholAc, only one peak could be clearly detected, while
230 amylopectin fraction is represented by a shoulder (Figure 2b) and the molar mass is
231 smaller for each elution volume. This accounts for the depolymerisation of amylopectin
232 by CholAc as well. When water was added to CholAc, a shift of amylopectin elution
233 toward higher volumes is still present, but again the overall behaviour is more similar to
234 that of pure water.

235 Table 2 shows \bar{M}_w values and \bar{R}_G obtained by integrating the signals for the whole
236 population of molecules present in the sample. A progressive and linear reduction in \bar{M}_w
237 is observed when EMIMAc concentration is increased, with a reduction % of 29, 48 and
238 80% for EMIMAc 50%, EMIMAc 70% and EMIMAc 100%, respectively, compared to
239 starch heated in pure water. Interestingly, when treated in CholAc, the reduction in \bar{M}_w
240 was non-linear, and reduction % were 25, 24, 27 and 81 for CholAc 60%, CholAc 70%,
241 CholAc 80% and CholAc 95%, respectively. The same trend was observed for \bar{R}_G . This
242 indicates that both ILs have a different response in the presence of water, with rather
243 small quantities of water (80%) reducing significantly the depolymerisation caused by
244 CholAc.

245 The dispersity (\bar{M}_w/\bar{M}_n) decrease for samples treated with ILs (from 7.56 to 7.10 and
246 4.48 for EMIMAc 100% and CholAc 95%, respectively) is linked to the reduction of the
247 overall peak broadness, and explained by the reduction of the amylopectin molar mass.

248 Although the two acetate based ionic liquid tested do not completely avoid starch
249 depolymerisation, the reductions of molar masses found in this study are very different
250 to those obtained after treating starches with halide based imidazolium IL, where
251 reductions of 1-3 order of magnitude can be observed.^{6,9,12}

252 From Table 2 it can be observed that a slight depolymerisation takes place when treating
253 starch with EMIMAc 50% and CholAc 60%, even though no exothermic transition was
254 observed by μ DSC. This finding may explain why gelatinization shifts to lower
255 temperatures and ΔH decreases when starch is heated in μ DSC with these IL-solutions,
256 since this mild depolymerisation may facilitate starch swelling shifting gelatinization
257 toward lower temperatures.

258 Moreover, the significantly lower molar masses observed for amylopectin populations
259 (Peak I, Figure 2) in EMIMAc 100% and particularly in CholAc 95% treated samples
260 compared to starch/pure water solutions account for a less dense structure (as these
261 fractions exhibit the same size because elution volume is proportional to size in HPSEC).
262 One can deduce that the original amylopectin population is linearized after heating in
263 ILs, and further in CholAc.

264 To sum up, it is clear that starch is depolymerized when heated in IL and that the
265 depolymerization pattern varies according to the cation nature, and not only to anion
266 characteristics. Though at present it is not possible to propose a mechanistic explanation
267 for this differential behavior, these results suggest the possibility of tailoring ionic liquid
268 for a controlled modification of starch macromolecular characteristics through mild
269 depolymerisation during destructureation.

270 The possible interaction between starch and IL during heating that could lead to the
271 formation of new molecular species was monitored by FTIR and NMR. No significant

272 changes were found between starch heated in water or ILs. These results can be collected
273 as Supplementary material (Figures S2 and S3).

274 It is also possible that the mechanism involves not only starch and LI, but also water
275 molecules. For future studies, a possibly fruitful approach for trying to understand the
276 interactions between these three components and their influence on the destructurement
277 mechanism would be the use of molecular simulation. A recent paper showed the
278 particular interest of this tool for understanding the interactions in the case of cellulose
279 dissolution in IL/water and IL/DMSO mixtures.²² It would also be interesting to study
280 the destructurement of starch in IL/DMSO mixtures, since these simulations show that
281 the co-solvent nature plays an important role in cellulose dissolution by IL.²²

282

283 **3.3. Microstructure of starch suspensions**

284 Figure 3 presents some representative images of corn starch heated in ILs solutions under
285 light and polarized-light (Figure 3a) microscopy, and differential interference contrast
286 and polarized-light (Figure 3b and c) microscopy. Figure 3a presents images of samples
287 before the enthalpic transition (depending on water content, endothermic or exothermic)
288 for starch suspensions heated in EMIMAc solutions where a well-defined granular
289 structure can be observed (similar images were obtained for CholAc, data not shown).
290 Images of starch suspensions after the enthalpic transition when heated in EMIMAc and
291 CholAc solutions are presented in Figure 3 (b,c). From these images, it can be observed
292 that when heated in pure water, starch granules are gelatinized: swelled, deformed and
293 with no remaining crystallinity. However, when EMIMAc is added (30 and 50%),
294 gelatinization is not complete, since some granules are still birefringent as a result of
295 their crystallinity. When EMIMAc reached 70%, however, no polarization was evident
296 after heating, and neither was the presence of granular remnants, and the same was

297 observed for EMIMAc 100%. The absence of granular remnants may indicate that starch
298 is not only depolymerized in concentrated EMIMAc solutions, but also it is solubilized.
299 Both phenomena, leading to an overall starch destructurement, may account for the
300 exothermic transitions observed by μ DSC. Figure 3c shows the same behaviour when
301 CholAc was used, but 80% of CholAc was necessary to achieve complete
302 destructurement, since at a lower concentration (70%) granular remnants were present.
303 Interestingly, starch suspended in EMIMAc 70% and CholAc 80% is completely
304 destructured at 56 °C and 92 °C, respectively, and under these conditions, only mild
305 depolymerisation is produced (Table 2).

306 When EMIMAc 100% and CholAc 95% were used, a few gas bubbles were observed
307 under the microscope. These gas bubbles may indicate the formation of volatile products,
308 but could not be identified.

309 These results are supported by images obtained with an Environmental Scanning Electron
310 Microscope –ESEM– for starch heated in pure water, pure EMIMAc and CholAc 95%. In
311 these images, the destructurement/solubilisation process is evidenced (Figure S4).

312

313 **3.3. Rapid Visco Analyser (RVA)**

314 RVA is an empirical study commonly performed on starch slurries to follow viscosity
315 behaviour as the sample is heated. While heated, the starch granules start to retain solvent
316 and swell, which results in a concomitant increase in viscosity, i.e. viscosity onset
317 temperature. The viscosity of the suspension increases to the point where the number of
318 swollen-intact starch granules is maximal. Peak viscosity (PV) is indicative of solvent-
319 binding capacity. Whereas the temperature increases and the granule absorbs as much
320 solvent as to achieve its rupture point, the viscosity decreases to a minimum. This
321 decrease in viscosity is called breakdown (BD). When starch suspension cools, amylose

322 retrogrades (re-crystallizes), resulting in an increase in viscosity named setback (SB),
323 until a gel is formed at the end of the test. In this study, viscosity onset temperature
324 correlated with μ DSC onset temperature, although the former was higher than the latter
325 (Tables 1 and 3).

326 It has been established that viscosity onset is higher than gelatinization onset
327 temperature,²³ since different techniques detect starch transitions in different ways
328 giving slight differences in the determined parameters.

329 Figure 4 presents the viscosity profiles of starch in EMIMAc (Figure 4a) and CholAc
330 (Figure 4b) solutions. ILs alone were also analysed, their viscosity was near zero and no
331 change in viscosity was observed during heating and cooling processes. From Figure 1
332 it can be seen that starch heated in concentrated EMIMAc solutions (100% and 70%)
333 undergoes an exothermic transition, related to starch depolymerisation/solubilisation;
334 and when EMIMAc was 50% or lower, an endothermic transition - ascribed to
335 gelatinization- took place. Figure 4a shows that when EMIMAc 100% is used, viscosity
336 increases as depolymerisation/solubilisation take place. During cooling stage, viscosity
337 increases significantly, probably as a consequence of the interaction between the
338 products of depolymerisation which are smaller and less branched than amylopectin,
339 favouring their association, and also to amylose retrogradation. As water is added
340 (EMIMAc 70%) the viscosity onset temperature and peak viscosity are lower (in
341 agreement with μ DSC results, Table 1). The decrease in the viscosity onset temperature
342 is related to the lower viscosity of the solvent when compared to pure EMIMAc, and its
343 diffusion into the granule which would be faster, facilitating depolymerisation.
344 However, starch depolymerisation is lower in EMIMAc 70%, explaining the lower
345 viscosity value during heating when compared to pure EMIMAc (Table 3). Increasing
346 the water content to 50% (EMIMAc 50%), the solvent diffusion into the granule

347 increases and the amount of water is enough to gelatinize starch. In addition, a slight
348 depolymerisation is also observed with EMIMAc 50% (Table 2). Both phenomena may
349 explain the higher viscosity shown by this sample (Table 3). When EMIMAc 30% is
350 used, the pasting behaviour is closer to that of starch in pure water, although overall
351 viscosity is higher. These results are in good agreement with Mateyawa *et al.*⁸
352 Figure 4b shows that starch in CholAc solutions have a different behaviour than in
353 EMIMAc solutions. When heated in concentrated CholAc solution (CholAc 95%) two
354 peaks are present: at the beginning of the test, CholAc is in solid state –explaining the
355 high viscosity of the sample at this point- but as temperature increases it melts; a second
356 increase in viscosity is observed during the cooling period. The exothermic peak
357 (observed by μ DSC) for this sample starts at around 97 °C (Table 1), this may explain
358 the absence of a viscosity peak during heating. However, some depolymerisation may
359 have occurred during the heating at 95 °C forming smaller and more linear molecules
360 from amylopectin, explaining the slight increase in viscosity during cooling. CholAc
361 70% could not be analysed since viscosity exceeded RVA limit (10000 cP).
362 For CholAc 50% and 30%, an increase in viscosity was observed between 85-90 °C (Table 3),
363 and no viscosity breakdown was found. The viscosity increase started late during heating, while
364 the maximum temperature reached by the RVA is 95 °C. This temperature may not be sufficient
365 to completely disrupt starch granular structure, although granules may swell and some amylose
366 may leach out, resulting in a viscosity increase.

367

368 **3.4. Phase diagram**

369 Summarizing, Figure 5 shows corn starch phase diagram when treated in different ILs
370 solutions. When IL concentration is high, complete loss of granular structure is observed
371 (result supported by microscopy images), and this destructure is accompanied by

372 starch depolymerisation (HPSEC-MALLS results), the degree of depolymerisation
373 depending on water amount. When water content is sufficiently high, gelatinization
374 occurs, instead of destructuration/solubilisation. Under these conditions, granular
375 remnants are still observed after heating. When EMIMAc 60% is used, a partial
376 gelatinization followed by partial destructuration/solubilisation takes place, and the
377 same is true for CholAc 70%.

378

379 **Conclusions**

380 Results presented in this study show that two different phenomena take place when
381 starch is heated in EMIMAc and CholAc solutions: when concentration of both ILs is
382 low enough, gelatinization is the dominating phenomenon, whereas when concentration
383 is higher, depolymerisation and dissolution of starch take place. The effect of both ILs
384 on gelatinization corresponds to that of stabilizing salts.

385 EMIMAc and CholAc have shown to be appropriate solvents for starch destructuration
386 when mixed with the correct amount of water (30% water for EMIMAc and 20% water
387 for CholAc). At these concentrations, destructuration (depolymerisation + dissolution)
388 starts at temperatures as low as 36 °C and 68 °C, respectively and, after heating at 120
389 °C, starch average molar mass is reduced by 27 and 48% when heated in CholAc 80%
390 and EMIMAc 70%, respectively. This suggest that specific starch chain breakings may
391 occur depending on the cation present in the IL, which could open the possibility of
392 solvent media design for a controlled modification of starch macromolecular
393 characteristics.

394

395

396

397 **Acknowledgements**

398 Authors gratefully thank the Région des Pays de la Loire for financial support. We would
399 also like to thank Bérénice Houinsou-Houssou for her kind technical support, and
400 Brigitte Bouchet, Bénédicte Bakan and Guillaume Roelens for their support in
401 microscopy, FTIR and ESEM analysis, respectively.

402

403 **Notes and references**

404 ^a LUNAM Université, CNRS, GEPEA, UMR 6144, CRTT, 37, Boulevard de l'Université,
405 44606 St Nazaire Cedex, France.

406 ^b UR1268 Biopolymères Interactions Assemblages, INRA, F-44300 Nantes, France.

407 ^c Structure Fédérative IBSM, INRA Nantes-Angers, Rue de la Géraudière, BP 71627,
408 44316 Nantes cedex 3. France.

409 Electronic Supplementary Information (ESI) available: [μ DSC, FTIR, ¹³C CP/MAS NMR
410 results and ESEM images are provided as Supplementary Material]. See
411 DOI: 10.1039/b000000x/

412

413 **References**

414 1 S. H. Ghaffar, M. Fan, *International Journal of Adhesion and Adhesives*, 2014, **48**, 92.

415 2 R. L. Shogren, G. F Fanta, W. M. Doane, *Starch/Stärke*, 1993, **45**, 276.

416 3 A. Buléon, P. Colonna, V. Planchot, S. Ball, *International Journal of Biological*
417 *Macromolecules*, 1998, **23**, 85.

418 4 N. Gathergood, P. J. Scammells, M. T. Garcia, *Green Chemistry*, 2006, **8**, 156.

419 5 T. G. A. Youngs, C. Hardacre, J. D. Holbrey, *Journal of Physical Chemistry B*, 2007,
420 **111**, 13765.

421 6 K. Lappalainen, J. Kärkkäinen, M. Lajunen, *Carbohydrate Polymers*, 2013, **93**, 89.

- 422 7 W. Liu, T. Budtova, *Carbohydrate Polymers*, 2013, **93**, 199.
- 423 8 S. Mateyawa, D. Fengwei Xie, R. W. Truss, P. J. Halley, T. M. Nicholson, J. L.
424 Shamshina, R. D. Rogers, M. W. Boehm, T. McNally. *Carbohydrate Polymers*, 2013,
425 **94**, 520.
- 426 9 D. G. Stevenson, A. Biswas, J. -L. Jane, G. E. Inglett, *Carbohydrate Polymers*, 2007,
427 **67**, 21.
- 428 10 A. Biswas, R. L. Shogren, D. G. Stevenson, J. L. Willett, P. K. Bhowmik,
429 *Carbohydrate Polymers*, 2006, **66**, 546.
- 430 11 K. Lappalainen, J. Kärkkäinen, J. Panula-Perälä, M. Lajunen, *Starch/Stärke*, 2012, **64**,
431 263.
- 432 12 J. Kärkkäinen, K. Lappalainen, P. Joensuu, M. Lajunen, *Carbohydrate Polymers*,
433 2011, **84**, 509.
- 434 13 V. Myllymäki, R. Aksela, 2005, WO Pat. No. 2005/066374A1.
- 435 14 J. F. Brennecke, R. D. Rogers, K. R. Seddon, In: *ACS symposium series*, 2007, Vol.
436 975 Washington DC: American Chemical Society.
- 437 15 P. Nockemann, B. Trijs, K. Driesen, C. Janssen, K. Van Hecke, L. Van Meervelt, S.
438 Kossmann, B. Kirchner, K. Binnemans. *Journal of Physical Chemistry B*, 2007, **111**,
439 5254.
- 440 16 A. Rolland-Sabaté, N. G. Amani, D. Dufour, S. Guilois, P. Colonna, *Journal of the*
441 *Science of Food and Agriculture*, 2003, **83**, 927.
- 442 17 V. Planchot, P. Colonna, L. Saulnier. (1997). In : B. Godon, W. Loisel (Eds.), *Guide*
443 *Pratique d'Analyses dans les Industries des Céréales*, Lavoisier (Paris, France), 1997,
444 341.
- 445 18 A. Rolland-Sabaté, P. Colonna, M. G. Mendez-Montevalvo, V. Planchot,
446 *Biomacromolecules*, 2008, **9**, 1719.

- 447 19 J. -L. Jane. *Starch/Stärke*, 1993, **45**, 161.
- 448 20 F. B. Ahmad, P. A. Williams, *Journal of Agricultural and Food Chemistry*, 1999, **47**,
- 449 3359.
- 450 21 N. Koganti, J. R. Mitchell, R. N. Ibbett, T. J. Foster, *Biomacromolecules*, 2011, **12**,
- 451 2888.
- 452 22 J. -M. Andanson , E. Bordes, J. Devémy, F. Leroux, A. A. H. Pádua, M.F. Costa
- 453 Gomes, *Green Chemistry*, 2014, **16**, 2528.
- 454 23 C. G. Biliaderis. In: J. N. BeMiller, R. L. Whistler (Eds), *Starch: Chemistry and*
- 455 *Technology*, Academic Press (New York, USA), 2009, 293.
- 456
- 457
- 458
- 459
- 460
- 461
- 462
- 463
- 464
- 465
- 466
- 467
- 468
- 469
- 470
- 471

472 **Table 1.** μ DSC results for regular corn starch heated in ILs/water solutions.

Solvent	Transition	ΔH ($J g^{-1}$)	T_o ($^{\circ}C$)	T_p ($^{\circ}C$)	T_c ($^{\circ}C$)
0% IL (pure water)	Endo	11.9 \pm 0.2a	60.3 \pm 0.1b	67.2 \pm 0.0b	73.3 \pm 1.4d
10% CholAc	Endo	13.7 \pm 0.0b	72.5 \pm 0.5c	78.4 \pm 0.1c	84.6 \pm 0.4ef
20% CholAc	Endo	14.3 \pm 0.9bc	77.5 \pm 0.2de	82.7 \pm 0.1d	86.7 \pm 3.4fg
30% CholAc	Endo	16.2 \pm 0.0d	80.3 \pm 0.5e	85.7 \pm 0.6d	89.8 \pm 0.1g
50% CholAc	Endo	16.2 \pm 0.5d	73.9 \pm 0.4cd	78.7 \pm 0.2c	83.1 \pm 0.1e
60% CholAc	Endo	14.4 \pm 0.9bc	58.7 \pm 4.7b	65.1 \pm 3.4b	69.6 \pm 2.6c
70% CholAc	Exo+endo	nd	46.7 \pm 0.2B	nd	66.9 \pm 0.8b
80% CholAc	Exo	39.5 \pm 1.4B	68.2 \pm 2.4E	78.4 \pm 1.4CD	88.4 \pm 1.9CD
90% CholAc	Exo	67.2 \pm 12.7C	85.9 \pm 1.1F	103.7 \pm 2.7E	114.3 \pm 3.4E
95% CholAc	Exo	nd	97.8 \pm 2.5G	nd	nd
10% EMIMAc	Endo	14.0 \pm 0.3b	70.7 \pm 1.0c	76.6 \pm 0.9c	82.9 \pm 0.8d
20% EMIMAc	Endo	14.7 \pm 0.4bc	73.1 \pm 0.4cd	78.4 \pm 0.2c	84.8 \pm 0.2ef
30% EMIMAc	Endo	15.5 \pm 0.3cd	72.9 \pm 0.4c	77.7 \pm 0.5c	83.7 \pm 0.3ef
50% EMIMAc	Endo	12.5 \pm 0.6a	51.5 \pm 0.3a	56.4 \pm 0.3a	62.9 \pm 0.9a
60% EMIMAc	None	nd	nd	nd	nd
70% EMIMAc	Exo	17.3 \pm 4.5A	36.2 \pm 0.8A	46.7 \pm 0.9A	52.2 \pm 0.6A
80% EMIMAc	Exo	63.3 \pm 2.3C	48.9 \pm 1.7B	65.0 \pm 1.9B	72.5 \pm 0.8B
90% EMIMAc	Exo	110.8 \pm 5.3D	56.2 \pm 0.5C	74.8 \pm 0.5C	85.7 \pm 0.8C
100% EMIMAc	Exo	180.7 \pm 20.8E	62.3 \pm 0.6D	80.1 \pm 0.3D	92.4 \pm 0.3D

473 ΔH : transition enthalpy; T_o , onset temperature; T_p , peak temperature; T_c , conclusion temperature.474 Values followed by different lowercase letters in the same column are significantly different ($p < 0.05$).475 Values followed by different uppercase letters in the same column are significantly different ($p < 0.05$).

476

477

478

479 **Table 2.** Weight-average molar mass (\bar{M}_w), dispersity (\bar{M}_w/\bar{M}_n) and z-average radius of gyration (\bar{R}_G)
480 \bar{R}_G) determined by HPSEC-MALLS for corn starch samples treated in ILs solutions.

Whole population			
Solvent	$\bar{M}_w (10^7)$ (g mol ⁻¹)	\bar{M}_w/\bar{M}_n	\bar{R}_G (nm)
Pure water	44.36±0.63	7.56±0.49	302.8±1.8
EMIMAc 50%	31.43±2.93	10.59±0.31	275.5±10.7
EMIMAc 70%	23.08±0.15	6.65±1.37	247.6±1.4
EMIMAc 100%	8.78±0.02	7.10±0.04	225.8±1.1
CholAc 60%	33.13±0.18	11.09±0.37	279.2±0.6
CholAc 70%	33.57±2.69	8.44±0.89	268.6±9.5
CholAc 80%	32.3±0.07	5.05±0.06	282.4±2.3
CholAc 95%	8.11±0.00	4.48±0.05	208.5±0.0

481

482

483

484

485

486

487

488

489

490

491

492

493

494

495 **Table 3.** RVA parameters for regular corn starch heated in ILs/water solutions.

Solvent	Peak viscosity (cP)	Trough (cP)	Breakdown (cP)	Final viscosity (cP)	Setback (cP)	Pasting temperature (°C)
0% LI (pure water)	1444±119a	1049±42ab	374±9b	2673±271b	1623±229a	72.5±0.5c
30% CholAc	2700±41b	2264±18d	nd	1740±27a	nd	90.9±0.8f
50% CholAc	5473±399d	4754±339e	nd	4332±721c	nd	84.9±0.1e
70% CholAc	nd	nd	nd	nd	nd	nd
95% CholAc	nd	nd	nd	nd	nd	nd
30% EMIMAc	3568±76c	1387±38bc	2181±38c	3994±76c	2607±38b	80.6±0.5d
50% EMIMAc	8249±20e	1548±20c	6701±0d	4289±62c	2742±42b	62.6±0.4b
70% EMIMAc	3071±95b	815±16a	2256±79c	3868±36.8c	3053±21c	55.7±0.9a
100% EMIMAc	2849±391b	2681±412d	168±22a	9939±308.6d	7255±105d	78.8±2.1d

496 Values followed by different lowercase letters in the same column are significantly different ($p < 0.05$).

497

498

499

500

501

502

503

504

505

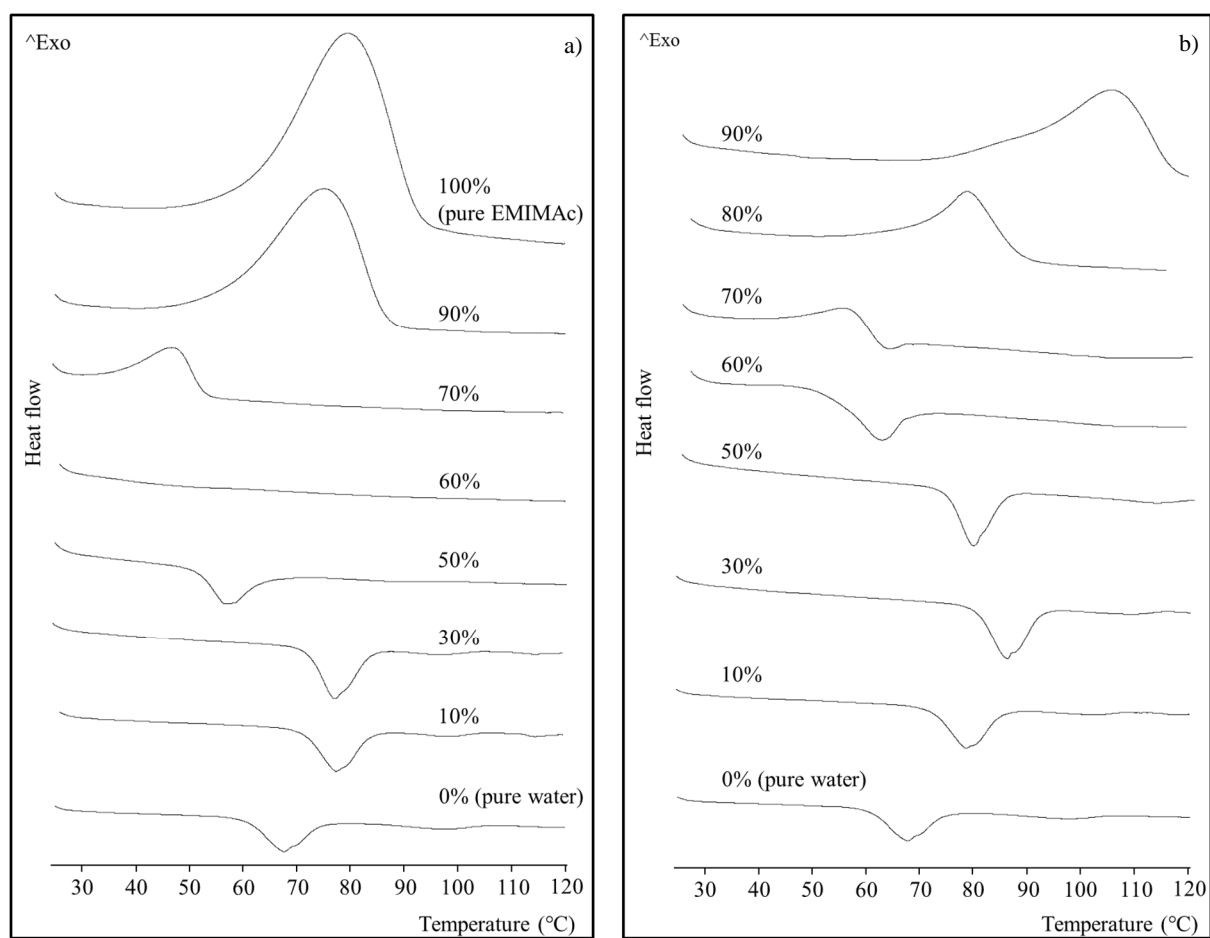
506

507

508

509

510



511

512 **Figure 1.** Micro differential scanning calorimetry thermograms for regular corn starch heated in

513 EMIMAc/water (a) and CholAc/water (b) solutions.

514

515

516

517

518

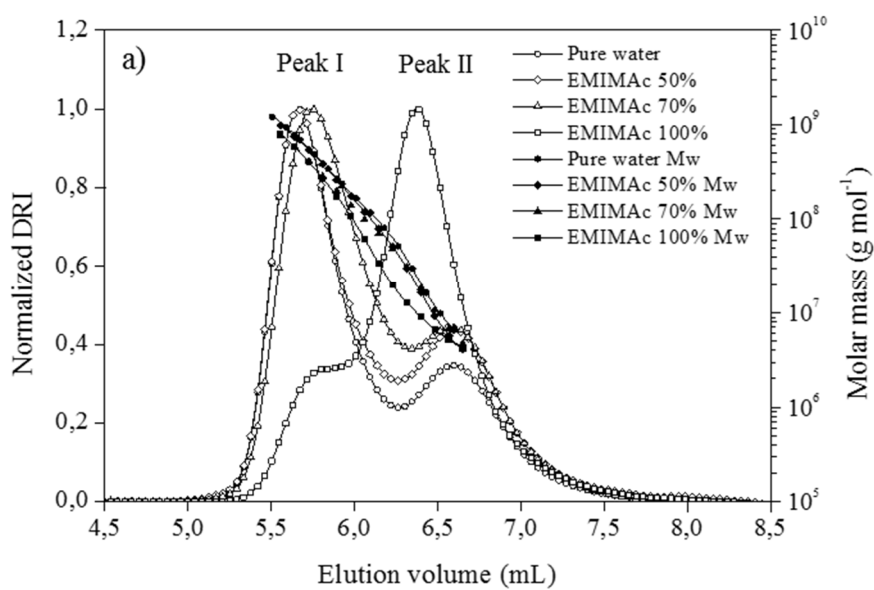
519

520

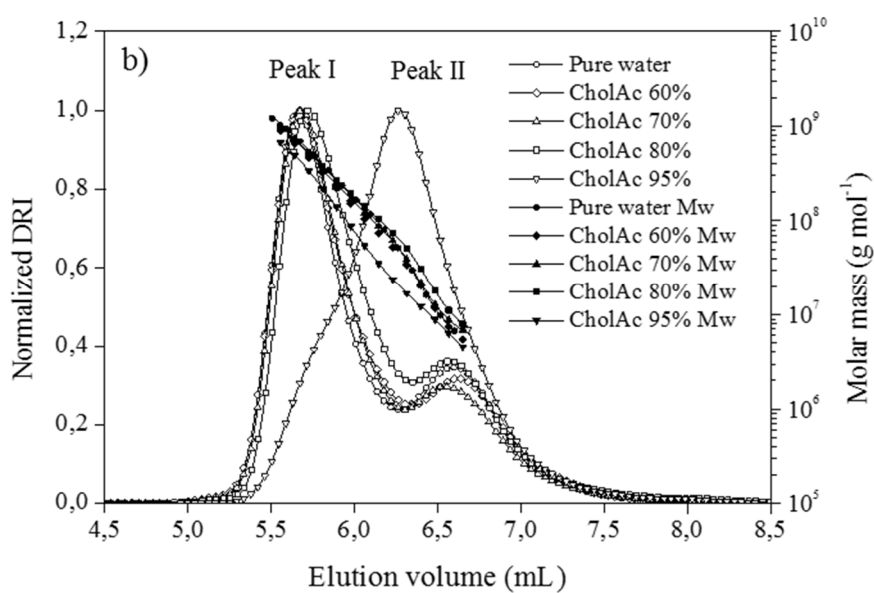
521

522

523



524



525

526 **Figure 2.** Chromatograms of regular corn starch treated with EMIMAc (a) and CholAc (b) solutions
 527 (differential refractive index –DRI- answer) and molar masses (M_w) versus elution volume.

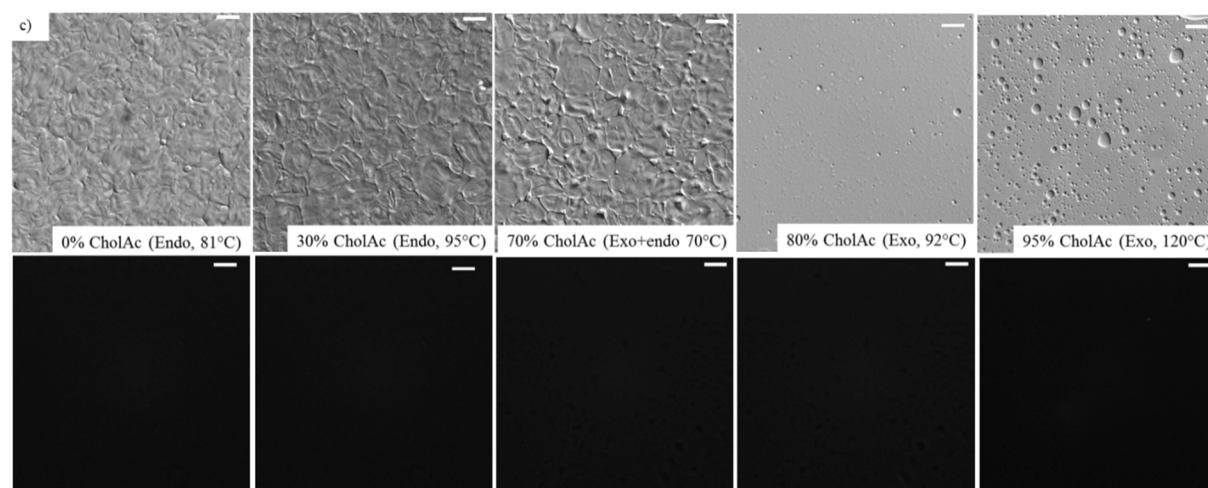
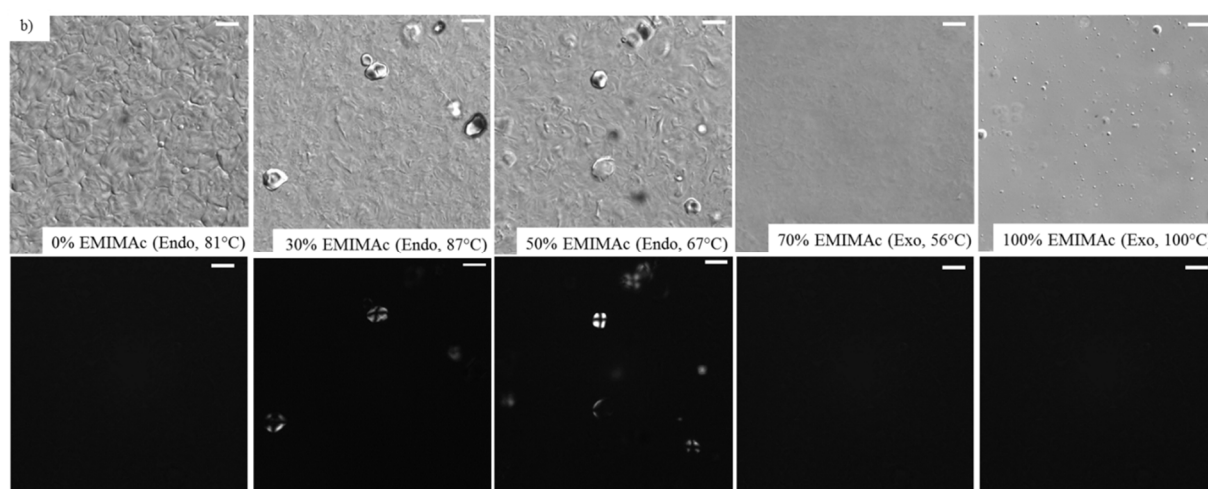
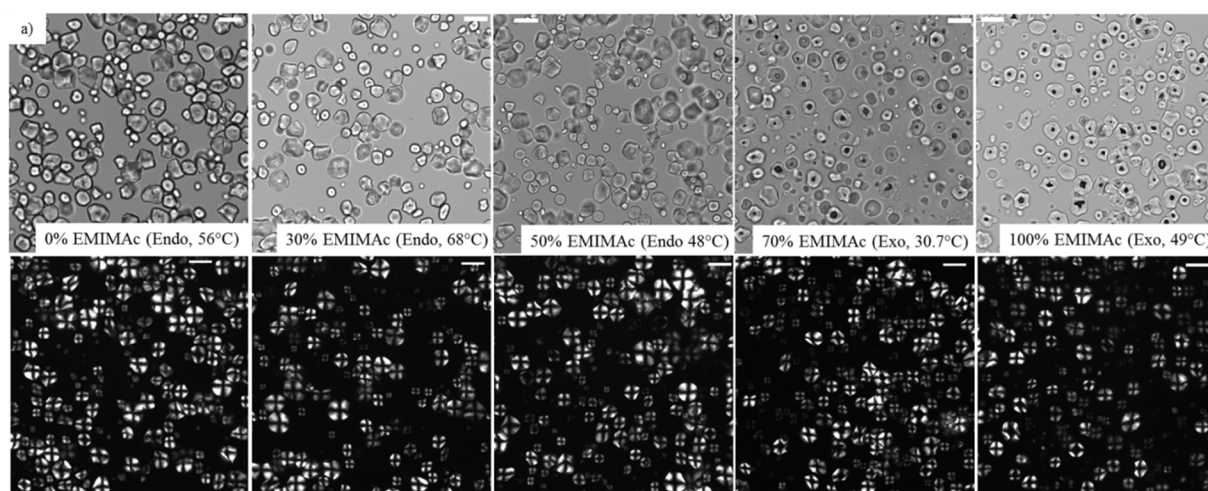
528

529

530

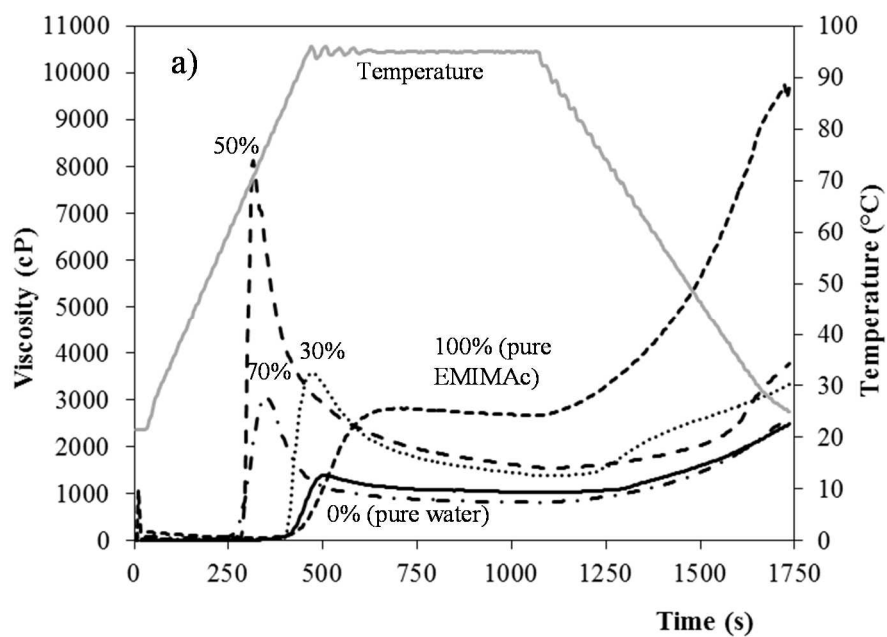
531

532

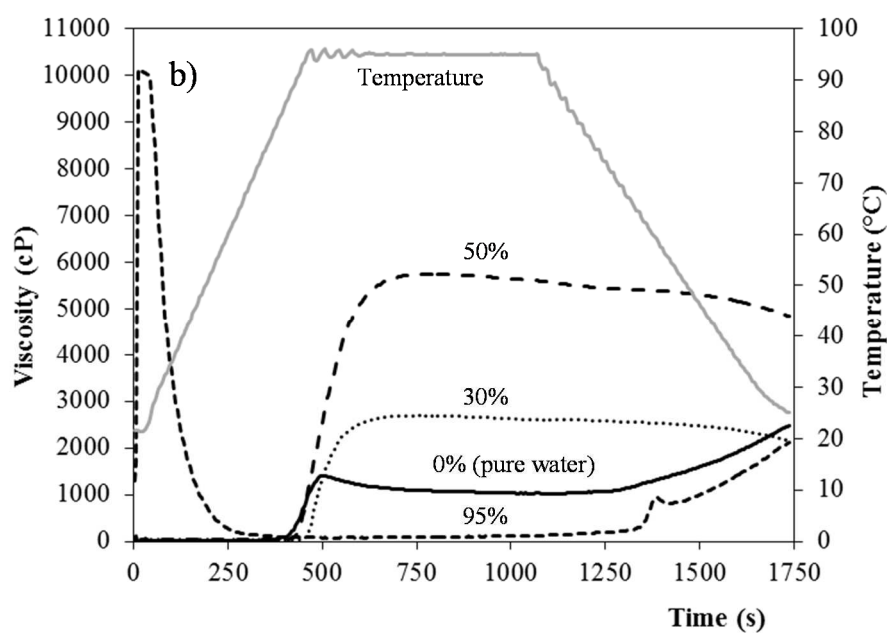


536 **Figure 3.** Light, polarized-light and differential interference contrast images for starch treated in ILs.
 537 (a) Light and polarized-light images of starch heated in EMIMAc solutions (To); (b) Differential
 538 interference contrast and polarized-light images of starch heated in EMIMAc solutions (Tc), and (c)
 539 Differential interference contrast and polarized-light images of starch heated in CholAc solutions (Tc).
 540 Bar scale: 20 μm .

541



551



563 **Figure 4.** RVA curves for starch heated in EMIMAc (a) and CholAc (b) solutions.

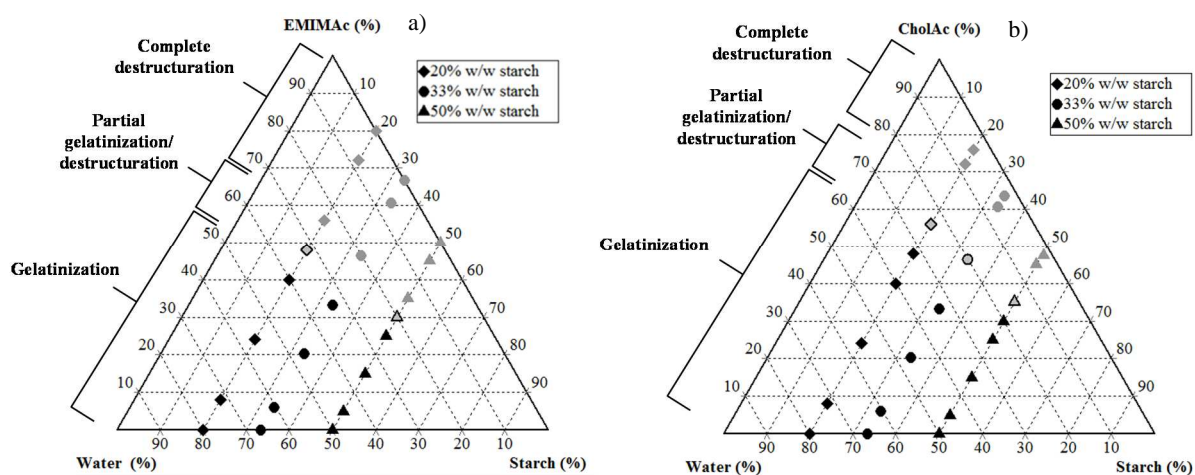
564

565

566

567

568



569

570 **Figure 5.** Phase diagrams for starch treated in solution with different ILs concentrations. (a) EMIMAc

571 treated starch, (b) CholAc treated starch.

572

573

574

575

576

577

578

579

580

581

582

583

584

585

586

587

588

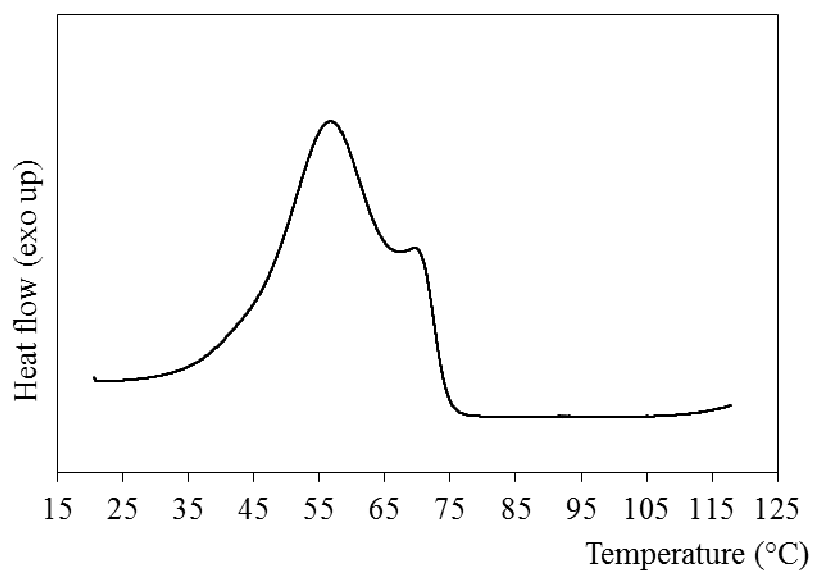
589

590

591

592 **Supplementary material**

593



594

595

596 **Figure S1.** μDSC curve starch heated in EMIMAc at 0.1 °C min⁻¹

597

598

599

600

601

602

603

604

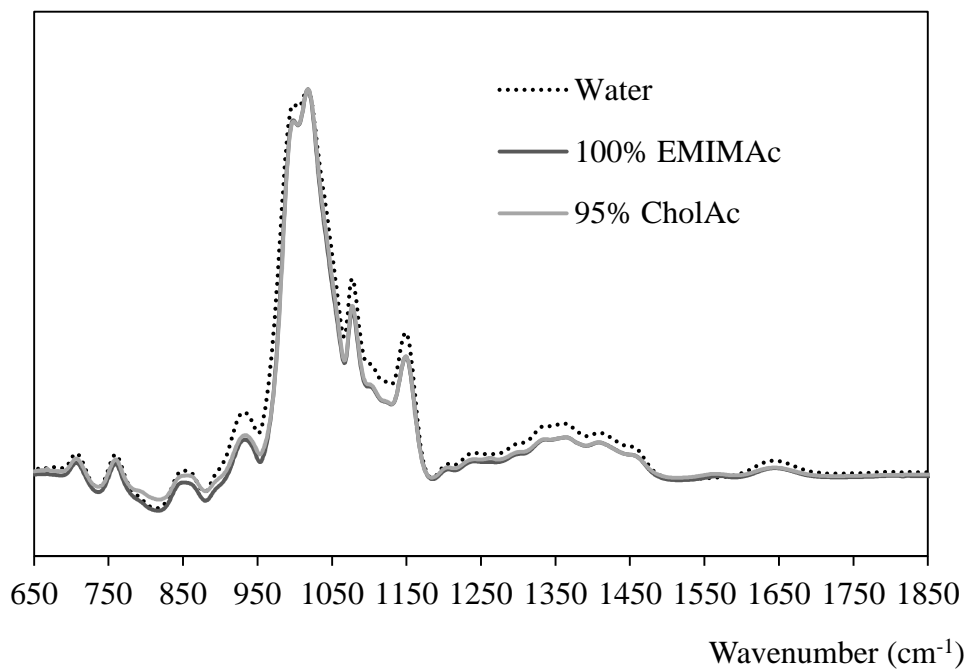
605

606

607

608

609



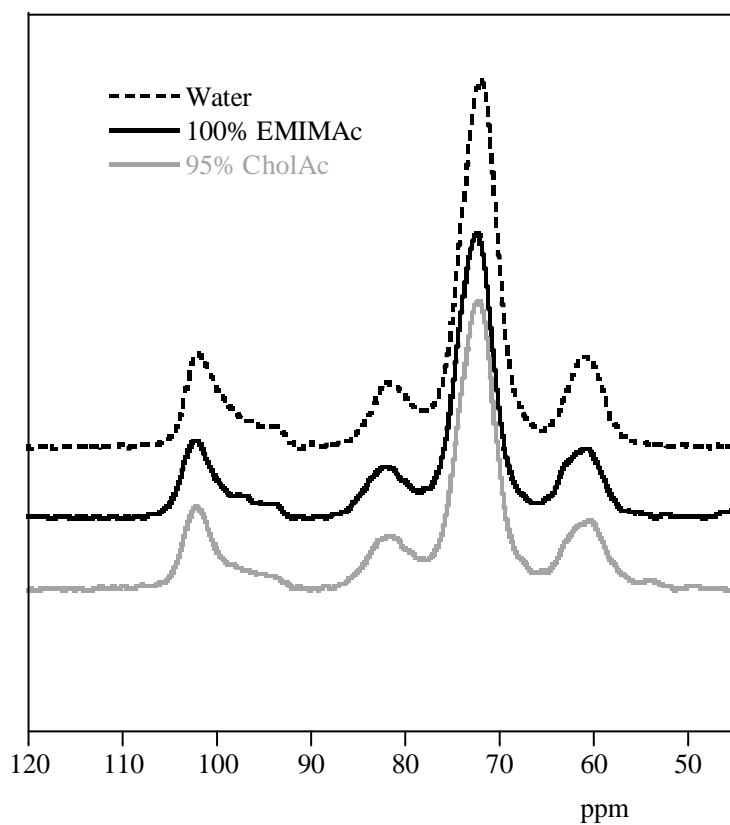
610

611 **Figure S2.** FTIR spectra of starch heated in pure water, EMIMAc 100% and CholAc 95% solutions.

612

613

614



615

616

617 **Figure S3.** ^{13}C CP/MAS NMR spectra of starch heated in pure water, and EMIMAc 100% and CholAc

618 95% solutions.

619

620

621

622

623

624

625

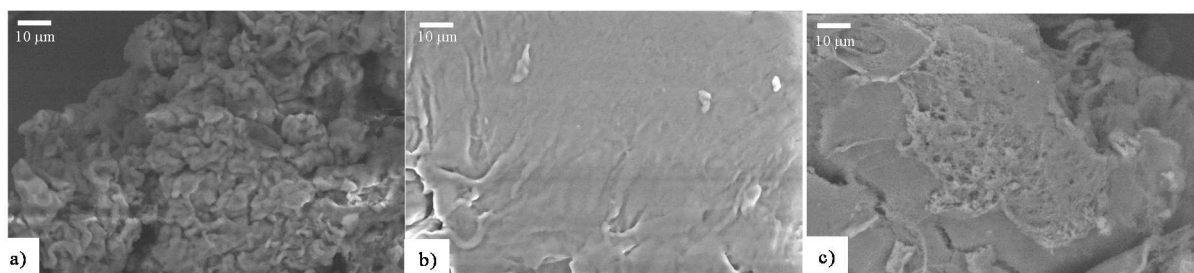
626

627

628

629

630



631

632 **Figure S4.** Environmental scanning electron microscopy (ESEM) images of corn starch heated in: pure
633 water (a), EMIMAc 100% (b), CholAc 95% (c).

634

635